Supporting Online Material for

γ-Secretase Heterogeneity in the Aph1 Subunit: Relevance for Alzheimer's Disease

Lutgarde Serneels, Jérôme Van Biervliet, Katleen Craessaerts, Tim Dejaegere, Katrien Horré, Tine Van Houtvin, Hermann Esselmann, Sabine Paul, Martin K. Schäfer, Oksana Berezovska, Bradley T. Hyman, Ben Sprangers, Raf Sciot, Lieve Moons, Mathias Jucker, Zhixiang Yang, Patrick C. May, Eric Karran, Jens Wiltfang, Rudi D'Hooge, Bart De Strooper[*]

*To whom correspondence should be addressed.
E-mail: bart.destrooper@med.kuleuven.be

This PDF file includes:

Materials and Methods
SOM Text
Figs. S1 to S7
Table S1
References

Materials and Methods

***In vitro* cell free γ-Secretase assay in triple *Aph1ABC* [-/-] cell lines reconstituted with the individual Aph1 components.**

The γ-secretase *in vitro* activity assay was performed as previously described (*1*) with minor modifications. Briefly, microsomal fractions from the different *Aph1*-deficient MEFs were suspended in a buffer (50 mM PIPES, pH 7.0, 0.25 M sucrose, 1 mM EGTA, complete PI (Roche)) at a protein concentration of 10 mg/ml. The membranes were solubilised with the addition of an equivalent volume of buffer containing 2% CHAPSO (Pierce) and incubated on ice for 1 h. After centrifugation at 100,000 x g for 1 h, the supernatant was used for the *in vitro* assay. APP C99-3xFLAG substrate was transiently expressed in Cos1 cells. γ-Secretase cleavage of the substrate was inhibited by the addition of an inhibitor (10µM GM6001, Sigma). Cells were harvested and resuspended in Tris-buffered saline (50 mM Tris-HCl, pH 7.6, 150 mM NaCl, 1% NP40, complete PI (Roche)) and incubated on ice for 1 h. After centrifugation at 245,000 x g for 20 min, the supernatant was incubated with anti-FLAG M2-agarose beads (Sigma). After several washes, APP C99-3xFLAG was eluted from the beads by incubation with 100 mM glycine HCl, pH 2.7 0.25% DDM (Sigma) and immediately neutralized (pH 7) by addition 1 M Tris-HCl, pH 8.0. For the reaction, the solubilised membranes were diluted 1:4 with CHAPSO-free reaction buffer (50 mM PIPES, pH 7.0, 0.25 M sucrose, 1 mM EGTA supplemented with EDTA free complete proteinase inhibitors (Roche), 0.8 µM of APP C99-3xFLAG, 2.5% DMSO, 0.1%l phosphatidylcholine and 0.0125% phosphatidylethanolamine (Sigma). AICD and Aβ production was analyzed after incubation at 37 °C for 3 h. Specificity of the

reaction was validated using a γ-secretase inhibitor (L-685,458, Calbiochem). To visualize

AICD, lipids and substrate in the reaction were first extracted with chloroform/methanol

(2:1). Semi-quantitative immune blot analysis using the anti-FLAG M2 antibody (Sigma)

and IR detection (Odyssey) was then performed using a known amount of substrate as a

standard. Aβ peptides were analyzed by urea-based Aβ SDS-PAGE and immune blot (2)

using 82E1 (Demeditec Diagnostics), a monoclonal antibody specific for the N-terminus of

Aβ or 1E8, another N-terminus specific monoclonal antibody (2). Signals were detected

using ECL chemiluminescence. $ELISA_{x-40}$ (the Genetics Company) and $ELISA_{1-42}$

(Biosource) were performed according the manufacturer's recommendations. The results of

these tests were compared using 2-way ANOVA analysis interaction between the pattern of

Aβ species and the γ-secretase pool, and *post-hoc* tests were applied as necessary (Fisher

LSD p<0,05). Mean ± SD. Student's t-tests were two-sided.

Fluorescence Lifetime Imaging Microscopy (FLIM): PS1 conformation in intact in

triple *Aph1ABC*$^{-/-}$ cell lines reconstituted with the *Aph1A$_L$* or *Aph1B* component.

MEF cells expressing either Aph1A$_L$ or Aph1B were transiently transfected with wild- type

PS1. The conformation of the PS1 molecule (NTF-loop and NTF-CTF proximity) was

monitored using a Fluorescence Lifetime Imaging microscopy (FLIM) FRET assay as

previously described (3, 4). Cells were immunostained with antibodies directed against the

PS1 amino-terminus (NTF) alone (for the negative control) or antibodies against PS1 NTF

and carboxyl-terminus (CTF) using goat-anti-NTF and Rabbit-anti-CTF, respectively,

(Sigma), or against PS1 NTF and a monoclonal antibody directed against the

transmembrane domain 6-7 loop (Millipore). Corresponding secondary antibodies were

labeled with Alexa 488 (donor fluorophore) and Cy3 (acceptor fluorophore). A mode-locked femtosecond-pulsed Ti:Sapphire laser (Mai-Tai, Spectra Physics, CA) was used for two-photon excitation. Fluorescence lifetimes of the donor were recorded using a high-speed Hamamatsu detector (MCP R3809, Hamamatsu City, Japan) and a fast time-correlated single-photon counting acquisition board (SPC-830, Becker&Hickl, Germany) that allows high temporal resolution lifetime acquisition. Donor fluorophore (Alexa 488 or GFP) lifetimes were fit to single-exponential (for donor alone) or double-exponential (for donor and acceptor) decay curves. The first (longer) lifetime corresponds to the non-FRETing population as observed in no-acceptor negative control, and the second (shorter) lifetime reflects the FRETing population. The FLIM assay monitors lifetime of the donor fluorophore as a measure of proximity between Alexa 488 labeling of the PS1 NT and Cy3 acceptor fluorophore labeling of the PS1 TM6-7 loop domain or the PS1 CT. The donor fluorescence lifetimes are shorter in the presence of FRET, and the degree of lifetime shortening is an inherent quantitative measure of proximity. Thus, changes in this quantity reflect alterations in PS1 conformation. Statistical significance was determined using ANOVA Fisher's PLSD. Statistical significance was assessed at $p < 0.05$.

Generation of littermate control mice of the appropriate genotypes.

The $Aph1BC^{-/-}$ (Aph1B^{tm1Bdes}, Aph1C$^{tm1.1Bdes}$) (5) and $APPPS1-21$ (Tg(Thy1-APP$^{KM670/671NLjuc}$), Tg(Thy1-Psen1^{L166Pjuc})) mice (6) were crossed to obtain littermate control mice of the genotypes of interest, namely $Aph1BC^{-/-}$ and $Aph1BC^{+/+}$ mice in $APPPS1^{+/+}$ (homozygous) condition; $Aph1BC^{-/-}$ and $Aph1BC^{+/+}$ mice in $APPPS1^{+/0}$ (hemizygous) condition; along with control genotypes ($Aph1BC^{-/-}$ and $APPPS1^{+/+}$ in full wild type or $APPPS1^{0/0}$ condition). Genotyping was performed on genomic DNA using

conventional PCR amplification and gel electrophoresis for the *Aph1BC* genotype and for the presence of both transgenes as previously described (*5, 6*). The final APP genotype was determined using quantitative real-time PCR amplification (primers: 5'-AAAACGAAGTTGAGCCTGTTGAT-3' and 5'-ACTGACCACTCGACCAGGTTCT-3' and SYBR-green detection (10x qPCR MasterMix Plus for SYBRgreen, Eurogentec) in a 7000 Sequence Detection System (Applied Biosystems). Only mice which were fully genotyped were included for analysis. Animals in which the *Aph1B* and *Aph1C* gene did not co-segregate correctly were eliminated.

Behavioural tests

Female littermate mice of 7 months of age (median 6.5 months; range 4.8-7.6 months) were evaluated using a battery of behavioural tests (*APPPS1*$^{+/0}$;*Aph1BC*$^{+/+}$: N=23 ; *APPPS1*$^{+/0}$;*Aph1BC*$^{-/-}$: N=23 ; *APPPS1*$^{+/+}$;*Aph1BC*$^{+/+}$: N=6 ; *APPPS1*$^{+/+}$;*Aph1BC*$^{-/-}$: N=9 ; *APPPS1*$^{0/0}$;*Aph1BC*$^{+/+}$: N=4 ; *APPPS1*$^{0/0}$;*Aph1BC*$^{-/-}$: N=4). These mice were group-housed in standard mouse cages with wood-shaving bedding. Food and water were available *ad libitum* in temperature and humidity controlled rooms with a 12 hr light-dark cycle. Behavioural testing was performed during the light phase of the day by experimenters blinded for the genotype. This protocol was approved by the institutional ethical committee for use on the experimental animals. Basic motor skills were tested using a rotarod and grip strength measurement. Locomotor and explorative behaviour was tested in an open field paradigm, in an elevated plus maze and in a social exploration test. Circadian variation in activity pattern was analyzed in a 24 hr activity cage. Spatial learning and memory were tested in a standard Morris water maze with hidden platform. Additionally, afferent visual pathways were examined using visual evoked potential registration. Detailed description of

these tests can be found elsewhere (*7*). To assess the effect of retraining at a slightly more advanced age, *APPPS1* hemizygous mice were enrolled at 7 months (median 6.5 months; range 4.8-7.6 months) and 11 months (median 10,7 months; range 9.2-12.2 months). The results of these tests were compared using ANOVA analysis. *Post-hoc* tests were applied as necessary (Fisher LSD p<0.05). Mean ±SEM values are shown. Student's t-tests were two-sided.

Measurement of Aβ species and immune blot analysis

Brains of the mice with respective genotypes of the ages indicated (± 2 weeks) were dissected after transcardial perfusion with ice-cold PBS. One hemisphere was fixed by immersion in modified Bouin's fixative and one was dounce homogenised in 2% SDS in H2O containing protease inhibitors (0,7 mg/ml Pepstatin A supplemented with a Mini complete protease inhibitor tablet, Roche). The homogenates were centrifuged at 4°C for 1 hr at 100,000 x g and the supernatants used for ELISA (the Genetics Company) and SDS-PAGE immune blot (10% and 4-12% Bis-tris, Invitrogen). Total protein concentrations were determined using the BCA protein assay (Pierce) and were used to determine the amount to load for SDS-PAGE, ELISA, or AlphaSreen assays. Antibodies used include 6E10 (against $A\beta_{1-17}$, Sigma), WO2 (against $A\beta_{5-8}$, the Genetics Company), 22C11 (against APP_{66-81}, Chemicon), a polyclonal APP C-terminal antibody (in-house) and β-actin (Sigma). Signals were detected using ECL chemiluminescence or IR detection if possible (Odyssey) and quantified relative to the signal of the β-actin control signal. $ELISA_{x-40}$ (the Genetics Company) and $ELISA_{1-42}$ (Biosource) were used according the manufacturer's recommendations. Endogenous mouse $A\beta_{x-40}$ and $A\beta_{x-42}$ from guanidine-HCl brain extracts

and CSF were measured using AlphaScreen technology (Perkin Elmer) as described in (*8*). Endogenous mouse $A\beta_{x-40}$ and $A\beta_{x-42}$ from 5 M guanidine-HCl brain extracts were measured by ELISA essentially as described in (*9*) with the following modifications: 1) the guanidine homogenates were diluted 1:6 rather than 1:10 to account for the lower expression levels of endogenous Aβs, and 2.) the ELISAs were re-configured in order to measure endogenous murine Aβ by using C-terminal specific capture antibodies (2G3 for Aβ40, and 21F12 for Aβ42) and biotinylated m266 as the detection antibody. Results shown are mean ± SEM.

Amyloid plaque load

Amyloid plaque load was measured in brains from 9 month old mice in 5 serial sagittal plane sections (8 μm) with a known intersection thickness (80 μm) after fixation and paraffin embedding (every tenth serial section is mounted on a glass slide). The slides were numbered and a slide number was randomly chosen. These slides were then processed simultaneously and stained for amyloid plaques using immunofluorescence with an Aβ-specific primary antibody (6E10, against $A\beta_{1-17}$, Sigma), after epitope exposure using 70% formic acid. Antibody-antigen complexes were revealed using an HRP-labelled secondary antibody and TSA™-Plus Fluorescein amplification (PerkinElmer). Bisbenzimide (Sigma) was used as counterstain. Controls included omission of the primary and secondary antibody (not shown). Digital images were taken simultaneously on a Zeiss Axiovert 200M microscope equipped with a motorized XYZ-stage equipped and stereology software (packet written for KS300 software, Zeiss). The amyloid plaque load was estimated in the volume of cortex and hippocampus sampled between the sections in volume and volume

percentage using a stereological approach, the Cavalieri point-counting method. Results shown are mean ± SEM.

Notch related side effects

T-cell, B-cell and NK-cell subsets were studied by flow cytometry using a FACStar Plus (Becton Dickinson). Venous blood was taken from the animals by intracardiac puncture or tail-biopsy. Peripheral blood leucocytes were obtained after lysis of the red blood cells using NH_4Cl. In addition, spleen and thymus were dissected and single cell suspensions were prepared. Peripheral blood lymphocytes and single cell suspensions were labeled with FITC-, PE- or PerCP-conjugated antibodies directed against CD3, CD4, CD8, CD25, CD62L, B220, IgM, IgD, CD23, CD21, DX5 and NK1.1 (Pharmingen, Becton Dickinson; eBioscience, ImmunoSource and Caltag Laboratories). Results shown are means and scatter diagrams showing individual data points.

To analyze the expression levels of *Notch1* target genes, the hippocampi were dissected after transcardial perfusion with ice-cold PBS from male hemizygous mice of 9 months of age of the *APPPS1* $^{+/0}$; *Aph1BC* $^{+/+}$ (N=6) and *APPPS1* $^{+/0}$; *Aph1BC* $^{-/-}$ (N=7) genotype. Total RNA was prepared using Trizol® (Invitrogen) following product instructions; RNA quality was checked using gel electrophoresis. First strand cDNA synthesis was performed using Superscript II™ Reverse transcriptase (Invitrogen) and treated with DNase (TURBO DNA-*free*™, Ambion) following product instructions. Target sequences were PCR amplified and detected in real time by SYBR-green (10x qPCR MasterMix Plus for SYBRgreen I, Eurogentec) using a 7000 Sequence Detection System (Applied Biosystems). All samples were run in triplicate and controls included no-amplification (no reverse

transcriptase added during cDNA synthesis) and no-template control (no cDNA added). Target genes were amplified using the following primer sets: *HES1* (5'-AAACCAAAGACGGCCTCTGA-3' and 5'-GAAGAGGCGAAGGGCAAGA-3'); *HES5* (5'-GCTCAGTCCCAAGGAGAAAAAC-3' and 5'-AAGATGCGTCGGGACCG-3'); *ACSL1* (5'-AGGCTCTCCTGGGAATGGA-3' and 5'-TGCATCTTTAGTGTTTCTCGCC-3'); *Notch1* (5'-CGCCCGTGGATTCATCTG-3' and 5'-TGAGAATGATGCCCGCACT-3'). Three house-keeping genes were amplified in parallel: *β-Actin* (5'-ACCCACACTGTGCCCATCTAC-3' and 5'-AGCCAAGTCCAGACGCAGG-3'); *HPRT* (5'-GCTTTCCCTGGTTAAGCAGTACA-3' and 5'-GAGAGGTCCTTTTCACCAGCAA-3'); *TATA-box binding protein* (5'-GGCCTCTCAGAAGCATCACTA-3' and 5'-TTATGCTCAGGGCTTGGC-3').

Histology

To investigate a possible effect of Notch pathway inactivation in *Aph1BC*$^{-/-}$ mice, intestine and pancreas were analysed using standard H&E or PAS histology. It has been described that after γ-secretase inhibitor treatment intestinal and pancreas morphology becomes deranged. Due to inhibition of differentiation, goblet cells become too numerous and become metaplastic, leading to a failure of the intestinal mucosa with villus blunting and intraintestinal haemorrhaging. In the pancreas, decreased cellular adhesion of acinar cells is demonstrated. The intestinal and pancreas morphology in the *Aph1BC*$^{-/-}$ mice was totally indistinguishable from its wild-type counterparts, as evaluated by a blinded pathologist.

Expression of Aph1 mRNA

Quantitative Reverse Transcriptase PCR

To analyze the expression levels of *Aph1* genes, the hippocampi, prancreas, gut, spleen and thymus were dissected after transcardial perfusion with ice-cold PBS from female wild type mice (N=5). Total RNA was prepared using RNeasy kit (Qiagen) following product instructions, RNA quality was checked using gel electrophoresis. First strand cDNA synthesis was performed using Superscript II™ Reverse transcriptase (Invitrogen) and treated with DNase (TURBO DNA-*free*™, Ambion) following product instructions. Target sequences were PCR amplified and detected in real time by SYBR-green (10x qPCR MasterMix Plus for SYBRgreen I, Eurogentec) using a 7000 Sequence Detection System (Applied Biosystems). All samples were run in triplicate and controls included no-amplification (no reverse transcriptase added during cDNA synthesis) and no-template control (no cDNA added). Target genes were amplified using the following primer sets: Aph1AL (5'- ACGCCGGGAGCCTCTTT-3' and 5'-AATGAGCCACCATCAGCAGAT), Aph1AS (5'- GGGTGCCCTCCCGATCT-3' and 5'- GCAACCTGCACTGTCCAGAA-3'), Aph1B/C (5'-TCTTCACCATCGCCACCG-3 and 5'-ACACCAACCAGAAGAAAGCA-3'). The amplification of the target sequences was analyzed using the δδCT method, comparing target gene expression to the gene expression of three house-keeping genes (see above) and is shown as fold difference compared to the average expression in hippocampi. Results shown are mean ± SD compared to β-actin. The results of these tests were compared using ANOVA analysis, and *post-hoc* tests were applied as necessary (Fisher LSD, $p<0.05$). Mean ±SEM values are shown. Student's t-tests were two-sided.

In Situ Hybridization

Frozen mouse brain sections were cut at 14-μm thickness on a Leica cryostat, thaw-mounted on silane-coated Superfrost slides, and stored at -70°C until subjected to prehybridization. Sections were fixed in a 4% phosphate-buffered paraformaldehyde solution, permeabilized with 0.4% Triton X-100, and acetylated with triethanolamine/acetic anhydride (pH 8.0). After dehydration using an ethanol gradient, the sections were air-dried and stored at -20°C until use. Radioactive (^{35}S-UTP) labeled probes were generated by in vitro transcription from pGEMT (Promega) vector constructs containing cDNA fragments complementary to mouse Notch1 (Acc.Nr. NM_008714, nt. 6292-7253), mouse Aph1A (Add Acc.Nr. NM_146104), Aph1B (Add Acc.Nr. NM_177583), and mouse GFAP (Acc.Nr. NM_010277, nt. 459-1307). C1q-specific riboprobes were generated from B-chain-specific C1q cDNA (425bp long; Acc.Nr. X71127) cloned into pBluescript as described previously (*10*). After hydrolysis, probes were purified by sodium acetate precipitation and then added to the hybridization solution (3x SSC, 50 mM sodium phosphate, 10 mM DTT, 1x Denhardt's solution, 0.25g/liter yeast tRNA, 10% dextran sulfate, and 50% formamide) to a final concentration of 5×10^4 dpm/μl. Fifty-microliters of the hybridization solution was applied to each section. A coverslip was placed on each slide, and the slides were incubated for 14 h at 60°C. Slides were washed in 2x SSC for 20 min followed by 30 min RNase A treatment (20 μg RNase A and 1 unit/ml RNase T1 (Roche) in 10 mM Tris (pH 8.0), 0.5M NaCl, 1 mM EDTA) at 37°C. The slides were then washed at room temperature in decreasing salt concentrations (1x, 0.5x, and 0.2xSSC) for 20 min each, and at 60°C in 0.2x SSC for 1 h, followed by a final rinse at room temperature in 0.2x SSC and distilled water for 10 min. The slides were first exposed using Kodak X-

ray films for 48 hours. Following development with the Kodak D19 developer, the slides were then covered with Kodak NTB2 nuclear emulsion and stored in the dark at 8°C. After exposure for 14–21 days, the slides were developed with the Kodak D19 developer, fixed, dehydrated, counterstained by cresyl violet, and embedded in DEPEX. X-ray film analysis was conducted using the MCID image analysis system (Interfocus Imaging). The autoradiograms were digitized under constant light and camera conditions. Bright- and dark-field microscopic analysis of autoradiograms was performed with an Olympus AX-70 microscope and the Spot RT slider digital camera (Diagnostics Instruments).

Depletion of Aph1B containing γ-Secretase complexes prepared from human and mouse cortex.

Microsomal membranes were prepared from fresh or frozen post-mortem mouse brains or pooled biopsied human cortex samples (all were non-AD patients, verified by histopathological examination), using Teflon homogenizer in a 0.5 M sucrose PKM buffer (100mM potassium phosphate; 5 mM $MgCl_2$; 3 mM KCl; pH 6.5) and consecutive centrifugations (1st 10' 2500 rpm then twice 10' at 8000 rpm). These membrane preparations were aliquoted according to total protein content, pelleted at 100,000xg for 1hr and frozen. The membrane pellets were solubilised in a similar manner as described above. The immunoprecipitation was performed as described before (*11*), using a PS1 (a.a. 263-378, C-terminus, clone PS1-loop, Chemicon; or an in-house polyclonal anti-mouse PS1 antibody as described before (*5*)) or Aph1B antibody (in-house polyclonal antibody as described before (*5*)) or pre-immune serum. Consequently, both the precipitated (bound) as well as the supernatant (unbound) fractions were then used for the *in vitro* cell-free assay as described above, but at a final CHAPSO concentration of 0.5%. The results were compared

using 2-way ANOVA analysis interaction between the pattern of Aβ species and the γ-secretase pool, and *post-hoc* tests were applied as necessary (Fisher LSD p<0,05). Mean ± SD. Student's t-tests were two-sided.

Text

Neuronal expression of Aph1B/C

Northern blot data indicated relatively strong expression of *Aph1B/C* in the brain compared to *Aph1A* (*12*) while *in situ* hybridization histochemistry showed that *Aph1B/C* is widely and specifically expressed in neurons throughout adult mouse brain (Fig. S5) (*13*). Aph1A is also expressed throughout the adult mouse brain, predominantly, but not exclusively, in neurons. Aph1A expression is high in the cerebral cortex, dentate gyrus, hippocampus and cerebellum. While Notch1 expression is ubiquitously expressed at low levels throughout adult mouse brain, Notch1 displays mostly a non-neuronal expression pattern. Notch1 expression overlaps with GFAP, a marker for astrocytes. Areas of high Notch1 expression (white matter areas, glial borders of the brain, blood vessels, ventricular ependyma) also display higher levels of C1q, a marker for cells of the monocyte/macrophage lineage, which detects microglia and perivascular macrophages in the adult brain (*14*).

Results and Figures

Fig. S1
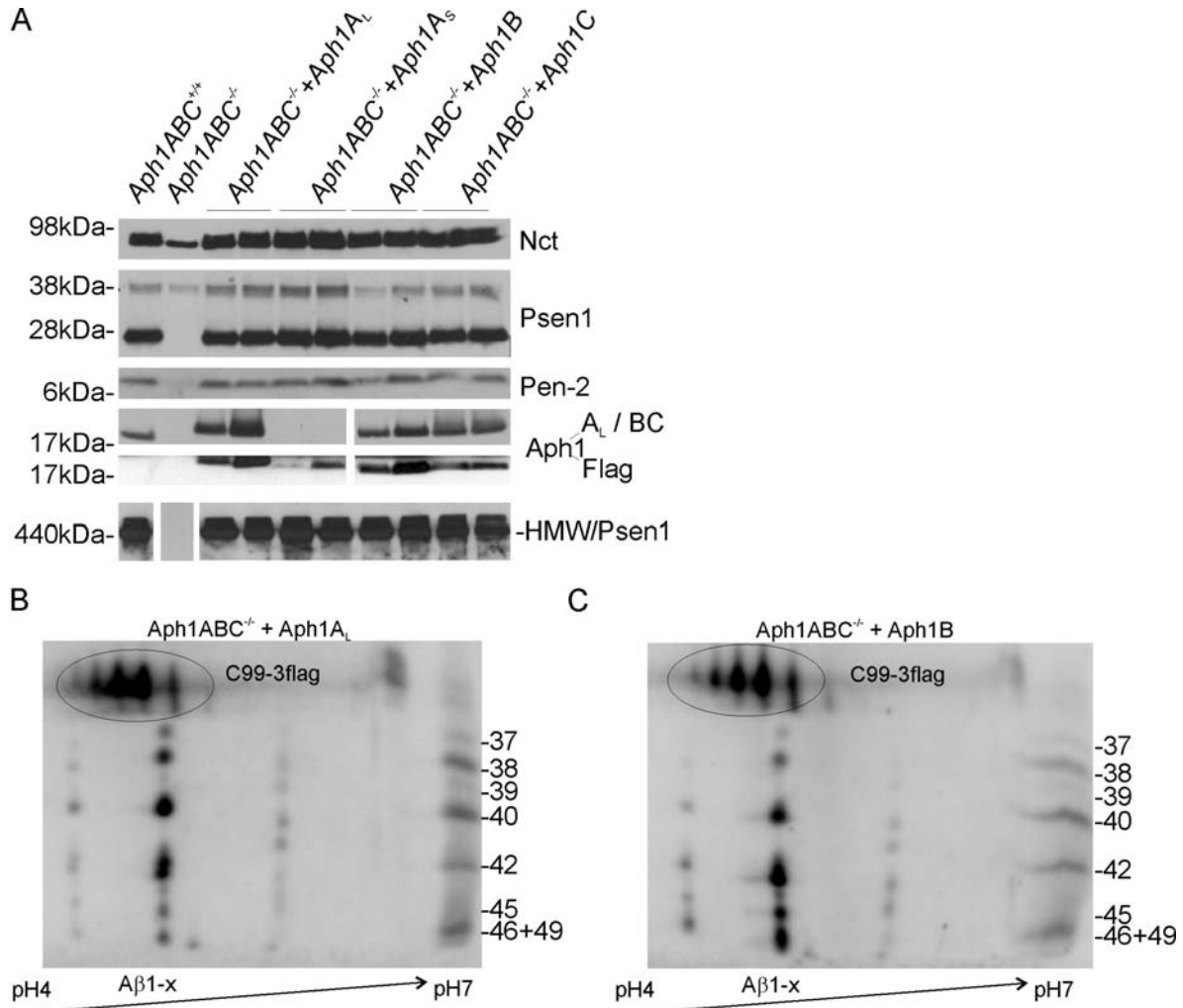
Fig.S1: All Aph1 homologues rescue the triple *Aph1ABC$^{-/-}$* phenotype but the Aph1 heterogeneity influences the γ-secretase cleavage sites. (A) *Aph1ABC$^{-/-}$* MEFs, were transduced with a single Aph1 homolog (Aph1A$_L$, Aph1A$_S$, Aph1B and Aph1C). Two independent cell-lines are presented. Membrane fractions from these cells were analyzed for the individual γ-secretase subunits by immunoblotting (Aph1aL with antibody B80,

Aph1B with antibody B78, NCT with antibody 9C3, PS1 with antibody B19 and Pen2 with antibody B126). *Aph1ABC*$^{+/+}$ wild type cells (lane 1) and *Aph1ABC*$^{-/-}$ cells (lane 2) served as controls. The lowest blot in the panel shows a Blue Native PAGE demonstrating that all MEFs express equivalent amounts of the high molecular weight γ-secretase complex (detected with antibody B19 against PS1). **(B, C)** Microsomal fractions of *Aph1ABC*$^{+/+}$ and *Aph1ABC*$^{-/-}$ MEF rescued with Aph1A$_L$ or Aph1B were solubilised with CHAPSO and incubated with 0.8µM C99-3xFLAG substrate at 37°C for 3h. Aβ species generated by Aph1A$_L$ or Aph1B γ-secretase complexes were dissolved in IPG rehydration buffer and separated by IEF on linear IPG strips (pH 4–7) and subsequently by urea-SDS-PAGE. Following transfer to PVDF membranes, the Aβ peptides were detected with the monoclonal 1E8 antibody. Synthetic standard Aβ peptides (run in 1-D separation) were loaded on the right side of each gel.

Fig. S2
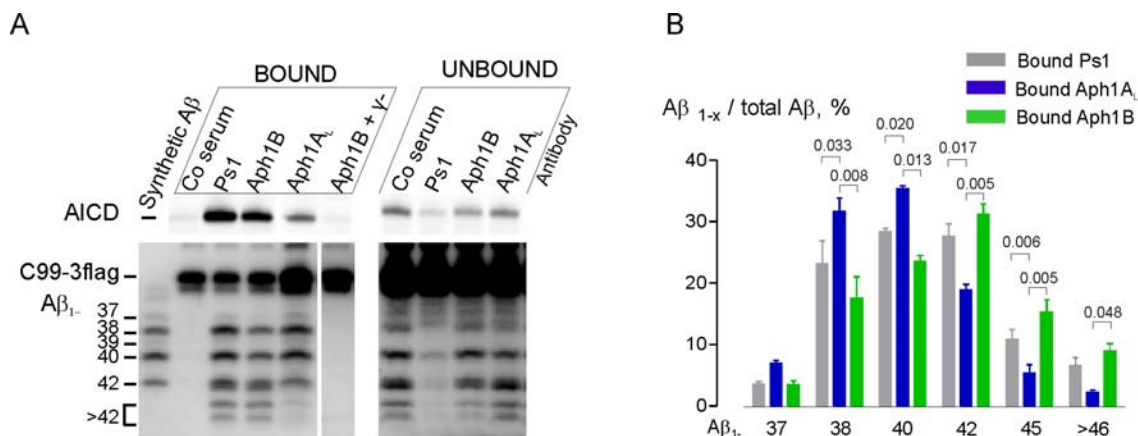
Fig. S2: Aph1B γ-secretase contributes to Aβ-production in mouse brain. (A) Following immunoprecipitation of microsomal membranes from wild-type mouse brain

tissue with pre-immune serum (Co serum), PS1-, Aph1B-, or Aph1A$_L$-specific antibody, γ-secretase activity was measured *in vitro* in both the bound and the unbound fractions, and AICD and Aβ species were measured. Comparison of the Aph1A$_L$ and Aph1B precipitated pools reveals a statistically significant shift in the pattern of Aβ production (mean±SD, n=3, p<0.05-0.01). **(B)** Quantification of the luminescence signal intensity, measured in the linear range of detection relative to the Aβ synthetic standard, and expressed as a ratio relative to the total Aβ signal per lane. Notice that 4x more sample was loaded for the Aph1A$_L$ bound sample. γ⁻: 10μM γ-secretase inhibitor L-685,458.

Fig. S3
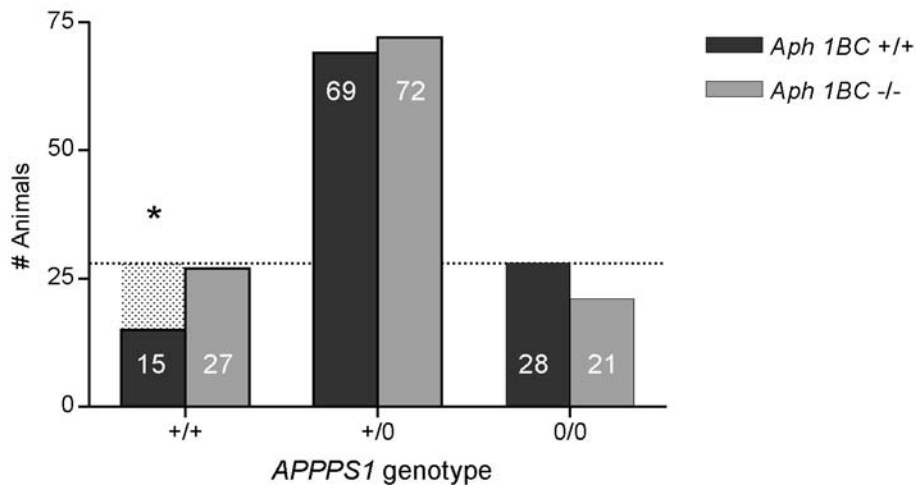
Fig. S3: Mendelian underrepresentation of the *APPPS1*^{+/+};*Aph1BC*^{+/+} mice. Mendelian underrepresentation of the *APPPS1*$^{+/+}$;*Aph1BC*$^{+/+}$ mice, compared to the *APPPS1*$^{0/0}$;*Aph1BC*$^{+/+}$ mice, as indicated by the dotted area was restored in the *APPPS1*$^{+/+}$;*Aph1BC*$^{-/-}$ mice (p<0,05, Chi-square test). The graph represents the number of offspring of the different *APPPS1* genotypes relative to the *Aph1BC* genotype.
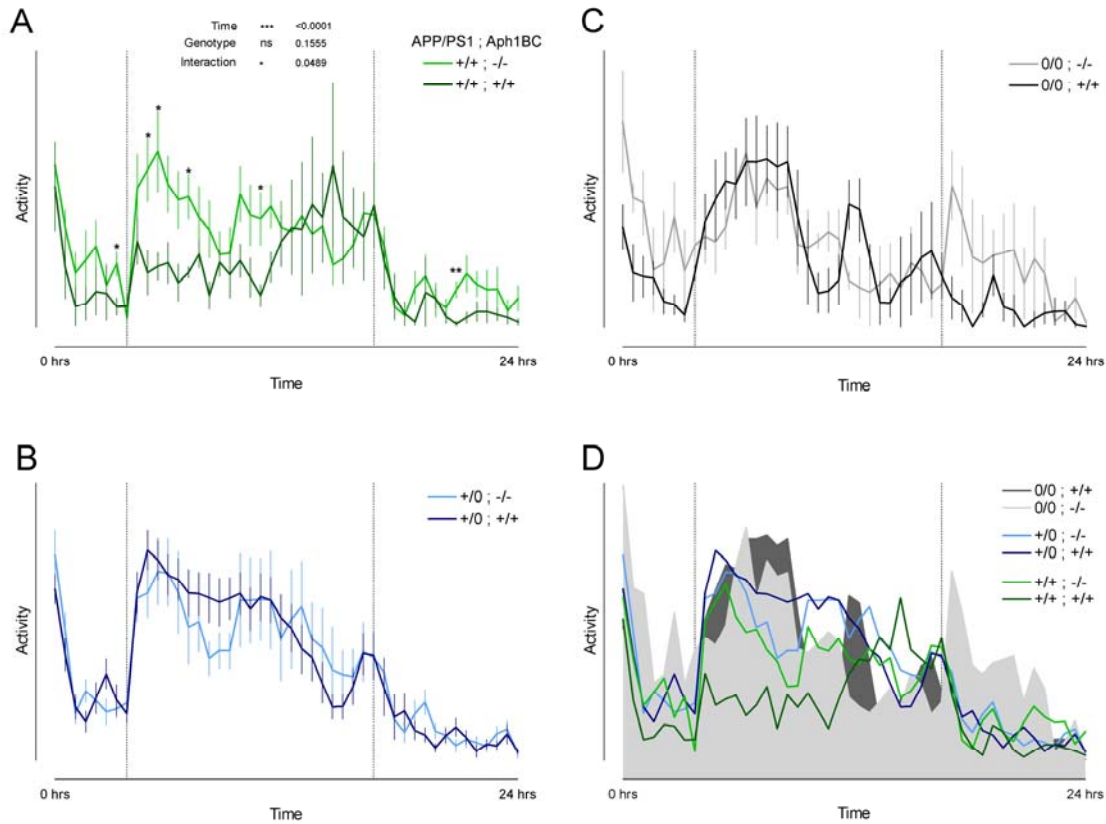
Fig. S4: The abnormal circadian activity pattern in the homozygous *APPPS1*^{+/+} mice is improved in the *APPPS1*^{+/+}; *Aph1BC*^{-/-} mice. Cage activity was monitored in groups of mice of the same age (median 5.6 months, range 3.9-6.6) and is represented as mean number of beam crossings ± SEM ('Activity') per 30 min episode ('Time') during the 24 hr recording period (lights off between the dotted lines, median age). **(a)** The abnormal circadian activity pattern in homozygous *APPPS1*^{+/+};*Aph1BC*^{+/+} mice was characterized by decreased overall activity and delayed acrophase (i.e. phase of peak activity) and may relate to activity changes in clinical AD (*14*). This altered activity pattern was significantly

improved in *APPPS1*$^{+/+}$;*Aph1BC*$^{-/-}$ mice (activity patterns were significantly different between the genotypes by 2-way RM ANOVA; genotype x time interaction $p < 0.05$; episodes where differences reached significance are indicated by asterisks, $p < 0.05$, $p < 0.01$, Fisher LSD test). **(b)** Hemizygous *APPPS1*$^{+/0}$ mice had a normal circadian activity pattern at this age regardless of their *Aph1BC* genotype **(c,d)** Wild-type patterns and cumulative graph.

Fig. S5
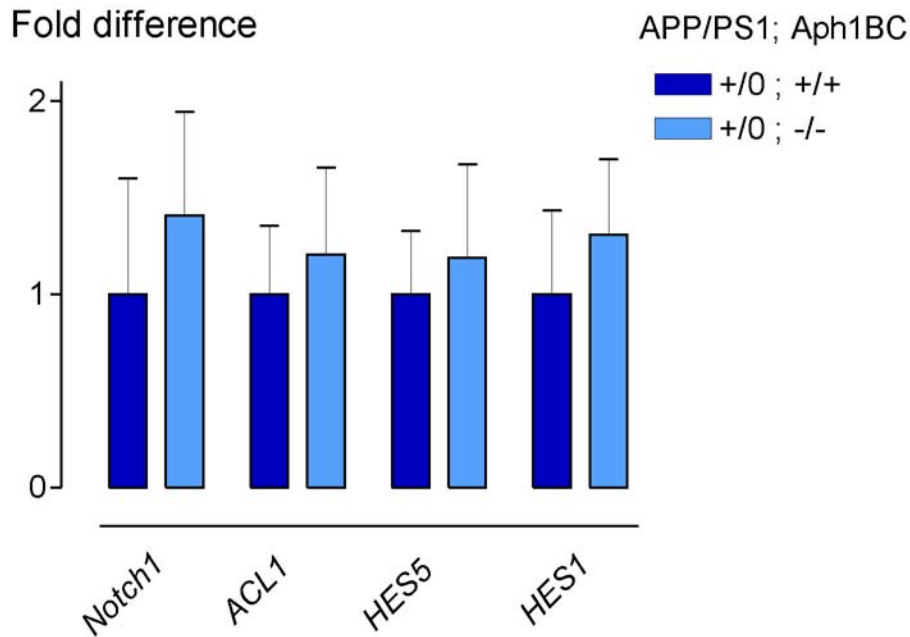
Fig. S5: No effects on Notch1 target genes expression in the brain of *Aph1BC$^{-/-}$* mice.

HES1, HES5, ACSL1 mRNA in hippocampi of *APPPS1$^{+/0}$;Aph1BC$^{+/+}$* (N=6) and *APPPS1$^{0/+}$;Aph1BC$^{-/-}$* mice (N=7) are not altered. Expression was normalized to the average expression of 3 house-keeping genes (*β-actin, HPRT, TATA box binding protein*) and is shown as fold difference compared to the average normalized *Aph1BC$^{+/+}$* expression (Mean±SD).

Fig. S6
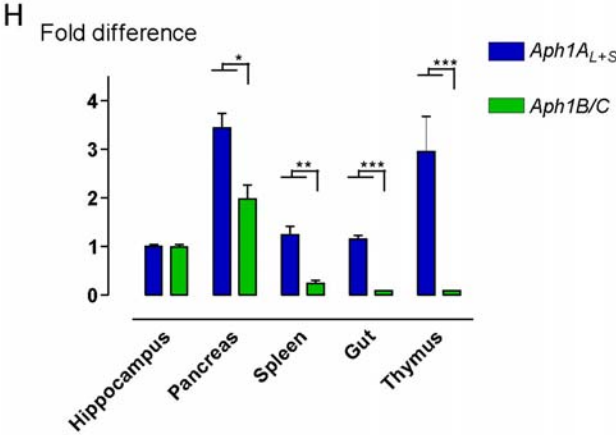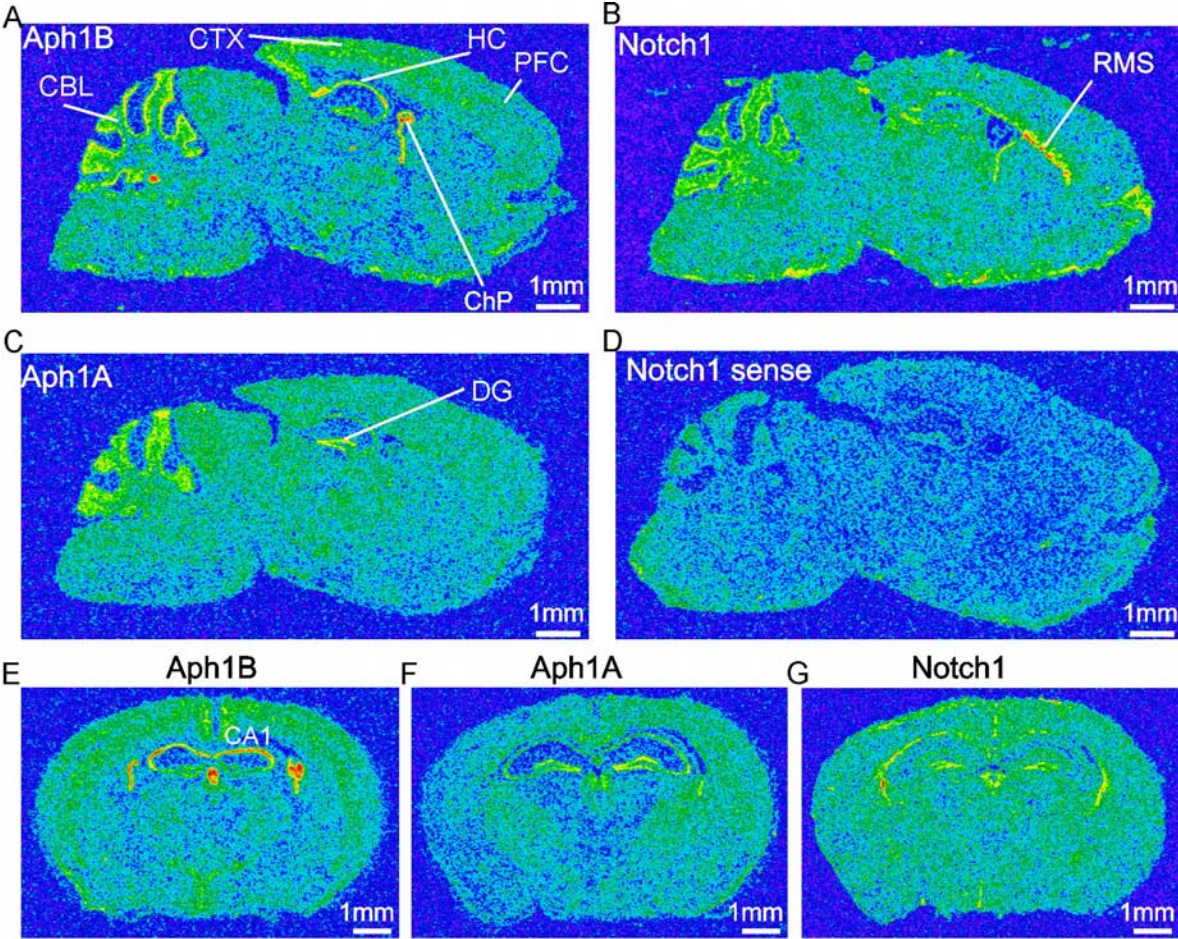
Fig. S6: Expression of Aph1B/C in neurons of the adult mouse brain. (A-D) Color-coded sagittal images of Aph1B/C, Aph1A and Notch1 mRNA in situ hybridizations on adult mouse brain using ^{35}S-UTP-labeled antisense (A-C) and sense (D) riboprobes. Note different distribution pattern of Aph1B/C and Notch1 mRNA in hippocampus (HC), prefrontal cortex (PFC), cerebellar cortex (CBL) choroid plexus (ChP) and rostral migratory stream (RMS). **(E-G)** Color-coded coronal images of Aph1B/C, Aph1A and Notch1 mRNA in situ hybridizations on adult mouse brain using the indicated antisense probes. Aph1B/C expression is high in the CA1 area of hippocampus and low in dentate gyrus (DG), while neuronal expression of Aph1A is highest in dentate gyrus. Notch1 is ubiquitously expressed throughout the mouse brain at low levels with higher expression restricted to non-neuronal areas lining the ventricles. **(H)** Relatively high mRNA levels of *Aph1B* (compared to *Aph1A$_L$* and *Aph1A$_S$*) in hippocampi and pancreas and relatively low *Aph1B* expression in spleen, gut and thymus. Expression was normalized to expression of β-actin. Normalisation to *HPRT and TATA box binding protein* revealed the same result (N=5, Mean±SD, p<0.05-0.001)

Fig. S7
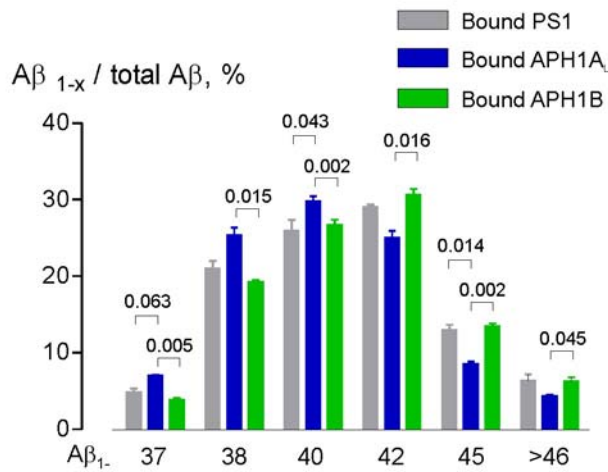
Fig. S7: Aph1B γ-secretase contributes to Aβ-production in human brain. Quantification of the luminescence signal intensity, measured in the linear range of detection relative to the Aβ synthetic standard, and expressed as a ratio relative to the total Aβ signal per lane.

Tables

Tab. S1

	Aph1BC$^{+/+}$			Aph1BC$^{-/-}$		
	$A\beta_{x-40}$	$A\beta_{x-42}$	$A\beta_{42}/A\beta_{40}$	$A\beta_{x-40}$	$A\beta_{x-42}$	$A\beta_{42}/A\beta_{40}$
Mean ± SE	ng/mg protein			ng/mg protein		
Hippocampus	278.4±15.9	91.1±58	0.334±0.070	200.3±14.9**	66.6±3.7**	0.347±0.075
Cortex	270.4±12.7	101.3±6.8	0.381±0.045	192.4±14.3***	77.8±4.5**	0.407±0.071

Tab. S1: Endogenous analyse of Aβ in hippocampal and cortical brain extracts from
***Aph1BC$^{+/+}$* versus *Aph1BC$^{-/-}$* mice.** Guanidine-HCl extractable $A\beta_{x-40}$ and $A\beta_{x-42}$ from mouse hippocampus and cortex was measured by ELISA (N=13, p<0.01).

1.	N. Kakuda *et al.*, *J Biol Chem* 281, 14776 (May 26, 2006).

2.	J. Wiltfang *et al.*, *J Neurochem* 81, 481 (May, 2002).

3.	A. Lleo, O. Berezovska, J. H. Growdon, B. T. Hyman, *Am. J. Geriatr. Psychiatry* 12, 146 (Apr 1, 2004).

4.	O. Berezovska *et al.*, *J. Neurosci.* 25, 3009 (Mar 16, 2005).

5.	L. Serneels *et al.*, *Proc Natl Acad Sci U S A* 102, 1719 (Feb 1, 2005).

6.	R. Radde *et al.*, *EMBO Rep* 7, 940 (Sep, 2006).

7.	H. Goddyn, S. Leo, T. Meert, R. D'Hooge, *Behav Brain Res* 173, 138 (Oct 2, 2006).

8.	P. G. Szekeres, K. Leong, T. A. Day, A. E. Kingston, E. H. Karran, *J Biomol Screen* 13, 101 (Feb 1, 2008).

9.	K. Johnson-Wood *et al.*, *Proceedings of the National Academy of Sciences of the United States of America* 94, 1550 (Feb 18, 1997).

10.	W. Schwaeble *et al.*, *J Immunol* 155, 4971 (Nov 15, 1995).

11.	S. S. Hebert *et al.*, *Neurobiol Dis* 17, 260 (Nov, 2004).

12.	S. S. Hebert *et al.*, *Neurobiology of Disease* 17, 260 (Nov 17, 2004).

13.	T. Dejaegere *et al.*, *Proceedings of the National Academy of Sciences* 105, 9775 (Jul 15, 2008).

14.	M. K. H. Schafer *et al.*, *J Immunol* 164, 5446 (May 15, 2000).